

# Binding of Autotaxin to Integrins Localizes Lysophosphatidic Acid Production to Platelets and Mammalian Cells\*

Received for publication, June 29, 2011, and in revised form, August 5, 2011. Published, JBC Papers in Press, August 10, 2011, DOI 10.1074/jbc.M111.276725

Zachary Fulkerson<sup>‡</sup>, Tao Wu<sup>‡1</sup>, Manjula Sunkara<sup>‡</sup>, Craig Vander Kooi<sup>§</sup>, Andrew J. Morris<sup>‡</sup>, and Susan S. Smyth<sup>‡¶2</sup>

From the <sup>‡</sup>Division of Cardiovascular Medicine, The Gill Heart Institute, <sup>§</sup>Department of Molecular and Cellular Biochemistry, University of Kentucky, Lexington, Kentucky 40536 and the <sup>¶</sup>Department of Veterans Affairs Medical Center, Lexington, Kentucky 40511

Autotaxin (ATX) is a secreted lysophospholipase D that generates the bioactive lipid mediator lysophosphatidic acid (LPA). We and others have reported that ATX binds to integrins, but the function of ATX-integrin interactions is unknown. The recently reported crystal structure of ATX suggests a role for the solvent-exposed surface of the N-terminal tandem somatomedin B-like domains in binding to platelet integrin  $\alpha\text{IIb}\beta_3$ . The opposite face of the somatomedin B-like domain interacts with the catalytic phosphodiesterase (PDE) domain to form a hydrophobic channel through which lysophospholipid substrates enter and leave the active site. Based on this structure, we hypothesize that integrin-bound ATX can access cell surface substrates and deliver LPA to cell surface receptors. To test this hypothesis, we investigated the integrin selectivity and signaling pathways that promote ATX binding to platelets. We report that both platelet  $\beta_1$  and  $\beta_3$  integrins interact in an activation-dependent manner with ATX via the SMB2 domain. ATX increases thrombin-stimulated LPA production by washed platelets  $\sim 10$ -fold. When incubated under conditions to promote integrin activation, ATX generates LPA from CHO cells primed with bee venom phospholipase  $A_2$ , and ATX-mediated LPA production is enhanced more than 2-fold by CHO cell overexpression of integrin  $\beta_3$ . The effects of ATX on platelet and cell-associated LPA production, but not hydrolysis of small molecule or detergent-solubilized substrates, are attenuated by point mutations in the SMB2 that impair integrin binding. Integrin binding therefore localizes ATX activity to the cell surface, providing a mechanism to generate LPA in the vicinity of its receptors.

tion, apoptosis, and development (1). In the cardiovascular system, LPA alters endothelial barrier function (2–4), modulates the phenotype of vascular smooth muscle cells (5), and is a weak platelet agonist (4, 6). Genetic and pharmacological approaches identify a role for LPA signaling in experimental models of vascular injury and atherosclerosis and suggest that responses of vascular cells to LPA observed *in vitro* are important *in vivo* (7–9). LPA, predominantly bound to serum albumin, is present in plasma at 0.5–1.0  $\mu\text{M}$  (10, 11). Plasma LPA is generated by hydrolysis of circulating lysophosphatidylcholine (LPC) catalyzed by the secreted lysophospholipase D, autotaxin (ATX) (12). ATX activity is required to sustain plasma LPA levels in the face of rapid elimination of this lipid from the circulation (13, 14). ATX potently stimulates the growth and migration of many cell types and is required for vascular development in mice. These functions clearly involve the production and actions of LPA; however, mechanisms regulating ATX activity to produce localized or cell-specific signaling responses are not well understood.

ATX belongs to a family of enzymes with ectonucleotide pyrophosphatase/phosphodiesterase activity (15). Among these ectonucleotide pyrophosphatase/phosphodiesterase activities, ATX (designated ENPP2) is unique in that it retains the characteristic activity of this class of enzymes against water-soluble nucleotide substrates but is also a lysophospholipase D (12, 16). ATX is a multidomain protein with tandem N-terminal somatomedin B-like (SMB1,2) domains, a catalytic phosphodiesterase domain (PDE), and a nuclease-like domain (15). The recently reported crystal structure of ATX reveals tight and extensive interactions between the PDE and nuclease-like domains and weaker interactions between the two SMB domains and the PDE domain. An extended hydrophobic substrate binding channel leading to the active site is formed in large part by the interface between the SMB and PDE domains. This channel appears to have arisen by deletion of sequences that are present in other ectonucleotide pyrophosphatase/phosphodiesterase activity proteins and, based on mutational studies and co-crystal structures, accounts for the unique selectivity of ATX for lipid *versus* small molecule substrates (17, 18). The introduction of mutations that block access to the channel reduces the ability of ATX to promote cell migration. These observations led to a proposed model in which the channel provides a conduit for cell surface localized generation of LPA and possibly also delivery of ATX-generated LPA to its G-protein-coupled receptors (18, 19).

Lysophosphatidic acid (1-acyl 2-hydroxyglycerol 3-phosphate (LPA))<sup>3</sup> is a bioactive lipid that binds to cell surface G-protein-coupled receptors to regulate cell growth, differen-

\* This work was supported, in whole or in part, by National Institutes of Health Grants GM050388 and RR026884 (to A. J. M.), HL078663 (to S. S. S.), GM094155 (to C. V. K.), and P2ORR021954 and F30 HL099272 (to Z. F.). This work was also supported by the resources and use of the facilities at the Lexington Veterans Affairs Medical Center.

<sup>1</sup> Supported by an American Heart Association postdoctoral fellowship.

<sup>2</sup> To whom correspondence should be addressed: Division of Cardiovascular Medicine, The Gill Heart Institute, 900 S. Limestone St., 326 CTW Bldg., Lexington, KY 40536-0200. Tel.: 859-323-3749; Fax: 859-281-4892; E-mail: SusanSmyth@uky.edu.

<sup>3</sup> The abbreviations used are: LPA, lysophosphatidic acid; ATX, autotaxin; LPC, lysophosphatidylcholine; PLA<sub>2</sub>, phospholipase A<sub>2</sub>; ANOVA, analysis of variance; SMB, somatomedin B-like; TRITC, tetramethylrhodamine isothiocyanate; TRAP, thrombin receptor activating peptide.

Several lines of evidence implicate platelets as important participants in LPA production in the circulation in some settings. LPA levels in serum prepared from platelet-rich plasma are ~5–10-fold higher than in platelet-poor plasma (20–22), which suggests that activated platelets play an active role in LPA production during clotting. Experimental induction of thrombocytopenia in rats, using an anti-platelet antibody, decreases the production of LPA in serum by almost 50% (20). Similarly, treatment of mice with a small molecule inhibitor of the platelet fibrinogen receptor, integrin  $\alpha\text{IIb}\beta_3$ , that causes thrombocytopenia significantly decreases circulating LPA (23). Although platelets themselves are clearly not a major source of ATX in the plasma, these observations raise the possibility that activated platelets or perhaps microparticles formed by activated platelets are a source of LPC substrate for ATX. Recent work identified acyl-protein thioesterase 1 (APT1) as being released during thrombin activation of platelets and is essential for platelet LPA production. The PLA<sub>1</sub> activity of APT1 generates *sn*-2 LPC on the outer surface of the membrane bilayer, which is proposed to undergo acyl migration to *sn*-1 LPC, and serves as a substrate for ATX (24). This process would necessitate that ATX localizes to the platelet surface. However, the mechanisms involved in cell localization of ATX and their importance for ATX-catalyzed production of LPA are presently unclear.

Activated integrins have previously been suggested to interact with ATX. ATX associates with activated platelets and accumulates in arterial thrombi through interactions with platelet integrin  $\alpha\text{IIb}\beta_3$  (11), and evidence for binding of ATX to additional integrin receptors on lymphocytes (25) and oligodendrocytes (26) has also been presented. Integrin activation could therefore serve as a mechanism to localize the recruitment ATX and spatially and temporally regulate LPA production. In this study we investigate integrin selectivity of ATX binding to platelets and mammalian cells and the regulation of this process by cell signaling pathways. Using antibody and small molecule inhibitors of the ATX integrin interaction and newly developed ATX mutants with impaired integrin binding, we demonstrate that recruitment of ATX to the surface of platelets and mammalian cells is a mechanism for localized LPA production.

## EXPERIMENTAL PROCEDURES

**Isolation of Recombinant ATX and ATX-derived Fragments**—cDNAs encoding wild type ATX, catalytically inactive ATX-T210A, an N-terminal ATX fragment containing amino acids 53–143, and various site-directed mutants were generated using standard methods inserted into a variant of pSecTag (Invitrogen) that was engineered for compatibility with the Gateway cloning system. Proteins were expressed by liposome-mediated transfection of these constructs in suspension cultures of Chinese hamster ovary (CHO) cells. Recombinant proteins were purified from filtration-concentrated CHO cell culture medium by nickel chelation chromatography as described previously (11).

**Preparation of Platelets**—Platelets were prepared using minor modifications of previously described methods (11). Citrated human blood was centrifuged at  $450 \times g$  for 5 min to yield

platelet-rich plasma, to which 134 nM prostaglandin I<sub>2</sub> was added. Platelets were separated from plasma by filtration of platelet-rich plasma, using a column of Sepharose 2B (Sigma) equilibrated in HEPES-buffered modified Tyrode's buffer (138 mM NaCl, 5.6 mM dextrose, 2.7 mM KCl, 10 mM HEPES, 12 mM NaHCO<sub>3</sub>, 0.36 mM NaH<sub>2</sub>PO<sub>4</sub>, pH 7.35) with 0.35% fatty acid-free bovine serum albumin (BSA; US Biological). For adhesion assays, platelet-rich plasma was incubated with 7  $\mu\text{M}$  calcein AM for 30 min at 37 °C prior to gel filtration. Unless otherwise indicated, gel-filtered platelets were diluted to 200,000/ $\mu\text{l}$  in Tyrode's buffer containing fatty acid-free (ethanol and charcoal-extracted) BSA (Sigma).

**Static Platelet/Cell Adhesion Assay**—Recombinant wild type ATX, ATX variants, or fibrinogen (American Diagnostica) diluted in Tris buffer (50 mM Tris, 100 mM NaCl, pH 7.4) were incubated in wells of a black polystyrene 96-well plate (Nunc) overnight at 4 °C. The wells were subsequently incubated for 1 h at room temperature with Tyrode's buffer containing BSA to block nonspecific binding sites. Calcein-labeled platelets or CHO cells (see above) were incubated for 1 h at 37 °C; nonadherent platelets were removed by washing Tyrode's containing BSA and 2 mM Ca<sup>2+</sup> and 1 mM Mg<sup>2+</sup>, or Mn<sup>2+</sup>, as indicated. The number of adherent platelets was determined by measuring fluorescence (excitation and emission = 494/517 nm) and reference to a standard curve generated by fluorescence measurements, using independently quantitated numbers of platelets. For analysis of platelet spreading and morphology, platelets were diluted to 20,000/ $\mu\text{l}$ , and adhesion was performed on LabTek2 coverslips. Adherent platelets were fixed with 4% paraformaldehyde, permeabilized, and stained with TRITC-phalloidin.

**Radioiodination of ATX**—ATX was radiolabeled using iodine-125 (<sup>125</sup>I) monochloride. 400–500  $\mu\text{g}$  of ATX was incubated with 2 M glycine and 0.231  $\mu\text{mol}$  of iodine monochloride/mg protein for 5 min on ice. <sup>125</sup>I-ATX was dialyzed overnight at 4 °C against PBS. Ninety five to 99% of the <sup>125</sup>I associated with the ATX was precipitated by trichloroacetic acid. <sup>125</sup>I-ATX was combined with platelets in the absence or presence of agonists and incubated at room temperature. Platelets were centrifuged at  $16,000 \times g$  for 30 s through 30% sucrose, and the amount of radioactivity associated with the platelet pellet determined (PerkinElmer Life Sciences, Packard Cobar II Auto-Gamma).

**CHO Cells**—CHO cells stably expressing human  $\beta_3$  integrin or  $\alpha\text{IIb}\beta_3$  were a generous gift from Zhenyu Li (University of Kentucky). For binding experiments, these cells were labeled with calcein using minor modifications of the method described for the platelets above. For measurements of LPA production by ATX, CHO cells were incubated with bee venom PLA<sub>2</sub> (Sigma) at concentrations of 0–10  $\mu\text{g}/\text{ml}$  for up to 60 min.

Determination of lyso-PLD activity was performed using detergent-solubilized substrates. ATX activity against 18:0 LPC was determined using a spectrophotometric coupled enzymatic assay with minor adaptations for use in a microplate reader (12).

**Measurement of LPA and LPC**—The lyso-PLD activity of ATX was measured in the absence and presence of platelets,

## Regulation of Autotaxin by Integrin Binding

stably transfected CHO cells, and purified integrins. We also measured LPC in some experiments. Lipids were extracted using acidified organic solvents as described previously. When measuring changes in endogenous lipids, the unnatural lipids 17:0 LPA or 17:0 LPC were added as an internal standard. In cases where production of C17 LPA by ATX-catalyzed hydrolysis of C17 LPC was measured, C17 sphingosine 1-phosphate was substituted as the recovery standard. The organic phase from these extractions was recovered, evaporated to dryness, and reconstituted in 100  $\mu$ l of methanol. Lipids (generally 10  $\mu$ l of each sample) were separated by reverse phase HPLC on an Agilent Zorbax C8 column and quantified by tandem mass spectrometry using an ABI 4000 Q-Trap hybrid linear ion trap triple quadrupole mass spectrometer. The mass spectrometer was operated in selective reaction monitoring mode to measure lipid species-specific precursor product ion pairs, with quantification accomplished by reference to calibration curves generated using synthetic standards obtained from Avanti Polar lipids that were independently quantitated by phosphorous analysis as described previously (13).

### RESULTS

**Synergistic Effect of Platelet Activation and ATX on LPA Generation**—The central role of ATX in production of circulating bioactive LPA has been established by a combination of genetic and pharmacological approaches. Very little is known about physiological mechanisms that may be responsible for regulating LPA production by ATX. Several observations suggest that platelets may serve as a useful model system to study regulation of ATX activity. Isolated platelets produce LPA after agonist stimulation in a process that appears to involve platelet release of APT1 and APT1-catalyzed generation of LPC, which presumably serves as a substrate for ATX. To confirm the role of ATX in platelet LPA generation, we tested the effects of a recently described potent small molecular inhibitor of ATX (13). A maximally effective dose of thrombin (0.5 units/ml) increased the LPA content of isolated platelets  $\sim$ 6-fold after 30 min. The thrombin-mediated increase in platelet-derived LPA was completely attenuated in a dose-dependent manner by the ATX inhibitor HA155 (Fig. 1A). Platelets contain immunologically detectable ATX (11), so these results indicate that ATX likely accounts for the previously reported ability of isolated human platelets to generate LPA in response to agonists (20, 28). Remarkably, thrombin-stimulated LPA generation by isolated platelets was dramatically increased when recombinant ATX was added to these incubations. The increase in LPA production was dependent on the concentration of added ATX with a half-maximal effect observed at concentrations of  $\sim$ 100 nM (Fig. 1B), which is in the range of the concentration of ATX reported in human plasma (29). When incubated with a maximally effective concentration of ATX, LPA generation by platelets was sustained at times up to 20 min (Fig. 1, C and D). The time course of LPA in the absence of added ATX or in response to a maximally effective concentration of ATX in the absence of agonist was biphasic, which may reflect the previously reported ability of platelets to degrade LPA (Fig. 1, C and D) (30). The low concentration of delipidated BSA in these incubations contained trace levels of lysophospholipids, including LPC, that

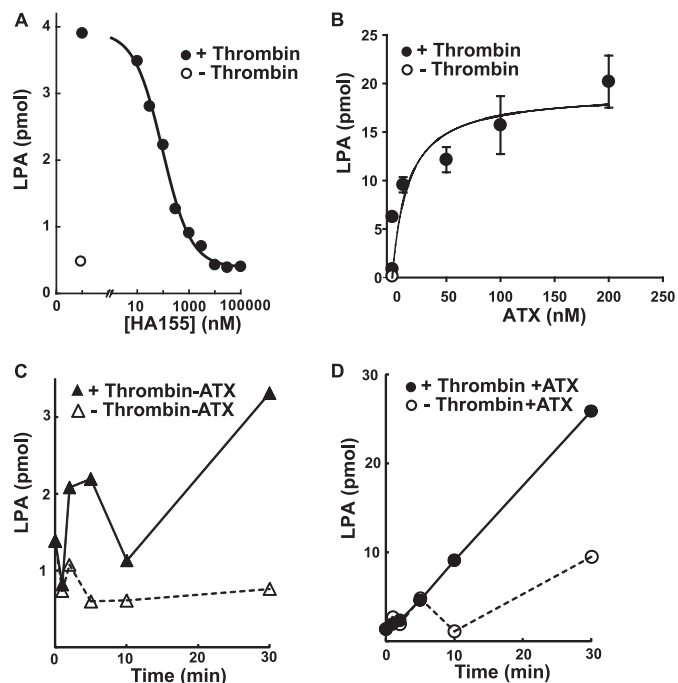


**FIGURE 1. Synthesis of LPA by thrombin-stimulated platelets is ATX-dependent and enhanced by exogenous ATX.** A, gel-filtered platelets were treated with vehicle ( $\circ$ ) or 0.5 units/ml thrombin ( $\bullet$ ) in the presence of the indicated concentrations of the ATX inhibitor HA155 for 30 min, and LPA was quantitated as described under "Experimental Procedures." B, LPA production by gel-filtered platelets was determined in the presence of vehicle ( $\circ$ ) or 0.5 units/ml thrombin ( $\bullet$ ) in the presence of the indicated concentrations of purified ATX and LPA quantitated as described under "Experimental Procedures." C and D, LPA production by gel-filtered platelets was determined at the indicated times in incubations containing no added ATX and vehicle ( $\Delta$ ) or 0.5 units/ml thrombin ( $\blacktriangle$ ) or 100 nM ATX and vehicle ( $\circ$ ) or 0.5 units/ml thrombin ( $\bullet$ ). Data shown are means of duplicate determinations (A, C, and D) or means  $\pm$  S.E. of triplicate determinations (B) from representative experiments that have been repeated using multiple independent preparations of platelets.

were not sufficient to sustain the quantities of LPA being formed. LPC was present in unactivated platelets ( $\sim$ 0.2 nmol/ $10^6$  platelets) and, presumably as a result of the recently described PLA<sub>1</sub> activity of APT1 (24), increased  $\sim$ 2-fold after stimulation with thrombin for 30 min in the presence of the ATX inhibitor. Taken together, our observations of sustained, amplified LPA production by thrombin-stimulated platelets in the presence of ATX suggest under these conditions ATX is acting on platelet-generated LPC, where substrate supply to the enzyme is not a rate-limiting determinant of LPA production.

**Signaling Pathways Regulating Binding of Platelet Integrins to ATX**—The ability of ATX to interact with integrin receptors could provide a mechanism for localizing the enzyme along the platelet surface. We therefore characterized ATX-platelet integrin interactions in more detail. LPA is a weak platelet agonist. To avoid confounding effects of ATX-generated LPA, we used a catalytically inactive mutant ATX-T210A to investigate agonist-dependent signaling pathways that regulate binding to platelets. Our earlier studies demonstrated that an antibody inhibitor of  $\beta$ 3 integrins blocked platelet adhesion to ATX (11). In agreement, echistatin, an RGD-containing peptide that competitively inhibits ligand binding to  $\beta$ 1 and  $\beta$ 3 integrins, dose-dependently reduced platelet adhesion to ATX-T210A to levels observed in unstimulated platelets (Fig. 2A). To investigate the

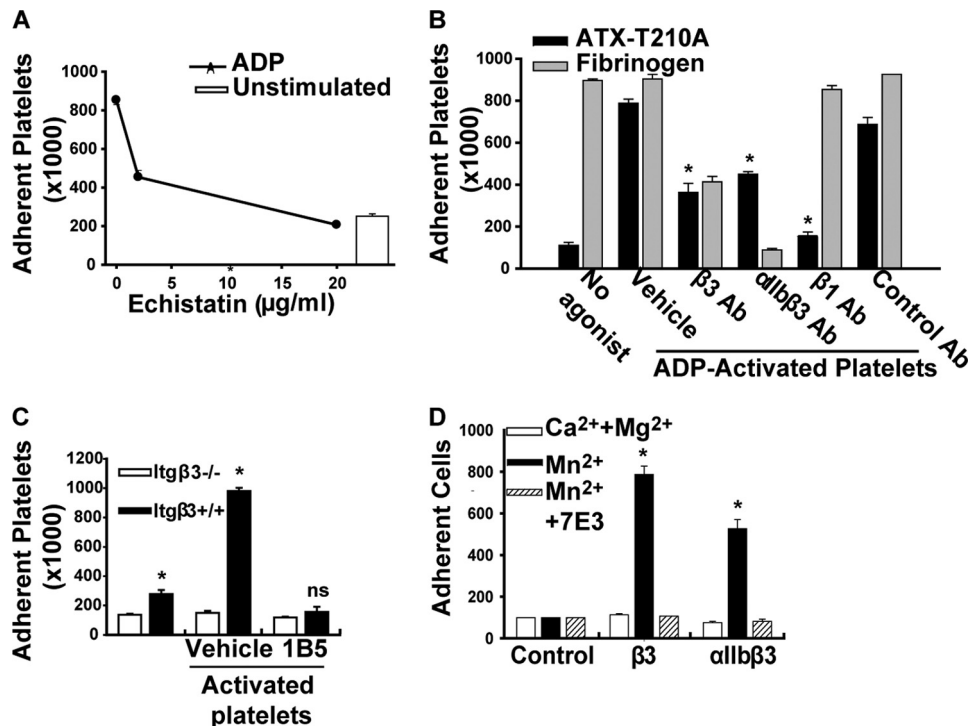


FIGURE 2. **Platelet adhesion to ATX requires  $\beta 1$  and  $\beta 3$  integrins.** *A*, platelet adhesion to microtiter wells with immobilized ATX-T210A without (open bar) or with 10  $\mu\text{M}$  ADP (●) and the indicated concentrations of echistatin, an RGD-containing disintegrin. *B*, results obtained with platelets from one donor incubated with wells containing immobilized ATX (dark bars) or fibrinogen (gray bars); immobilized at 10  $\mu\text{g}/\text{ml}$  in the presence of 10  $\mu\text{M}$  ADP and 20  $\mu\text{g}/\text{ml}$  of a function-blocking integrin  $\beta 3$  antibody (7E3), a function-blocking  $\alpha\text{IIb}\beta 3$  antibody (10E5), a function-blocking integrin  $\beta 1$  antibody (P4C10), or a nonfunction-blocking integrin antibody (23C6). *C*, platelets were isolated from wild type ( $\text{Itg}\beta 3^{+/+}$ ) or  $\text{Itg}\beta 3^{-/-}$  mice and incubated (200,000/ $\mu\text{l}$ ) with wells containing immobilized ATX in the presence of 150  $\mu\text{M}$  PAR4-activating peptide. Results are representative of those obtained in three separate experiments. \*,  $p < 0.05$  versus  $\text{Itg}\beta 3^{+/+}$  platelets, two-way ANOVA; ns = not significant. *D*, calcein-labeled CHO cells (300 cells/ $\mu\text{l}$ ) (control) or CHO cells that were stably expressing  $\beta 3$  or  $\alpha\text{IIb}\beta 3$  were incubated with immobilized ATX in the presence of 2 mM  $\text{CaCl}_2$  and 1 mM  $\text{MgCl}_2$  (open bars), 50  $\mu\text{M}$   $\text{Mn}^{2+}$  (black bars), or 50  $\mu\text{M}$   $\text{Mn}^{2+}$  and 20 mg/ml of the function-blocking integrin  $\beta 3$  antibody 7E3 (hatched bars). (\*,  $p < 0.05$  versus control CHO cells, ANOVA.) Results are presented as the number of adherent platelets or CHO cells (mean  $\pm$  S.D.) from triplicate determinations.

possibility that ATX-T210A can bind non- $\beta 3$  integrins on activated platelets, we used integrin function-blocking antibodies and compared responses to that of 7E3, an antibody inhibitor of  $\beta 3$  integrins that reduced adhesion by  $79 \pm 6\%$  ( $n = 8$ ). Monoclonal antibodies to integrin  $\alpha\text{IIb}\beta 3$  (10E5) and to  $\beta 1$  integrins (P4C10) also reduced adhesion of platelets to ATX-T210A by  $65 \pm 13\%$  ( $n = 4$ ) and  $87 \pm 6\%$  ( $n = 2$ ), respectively (Fig. 2*B*). The specificity of P4C10 was confirmed by the lack of effect on fibrinogen binding to platelet  $\beta 3$  integrins. LM609, a function-blocking  $\alpha\text{V}\beta 3$  antibody, had variable effects on the adhesion of platelets from three different donors to ATX-T210A, ranging from 1 to 62% inhibition (median inhibition 22%), which may reflect low and variable levels of platelet  $\alpha\text{V}\beta 3$  expression in platelets from different donors. Binding to ATX-T210A was substantially, but not completely, impaired in platelets from mice lacking  $\beta 3$  integrin ( $\text{Itg}\beta 3^{-/-}$ ). Murine platelet adhesion was inhibited by 1B5, a hamster monoclonal antibody to  $\alpha\text{IIb}\beta 3$  (Fig. 2*C*). Taken together, our results indicate that the association of ATX with platelets requires integrin activation and occurs through  $\beta 3$  and  $\beta 1$  integrins.

To determine whether  $\beta 3$  integrins were sufficient for supporting cell adhesion to ATX, we examined the effect of expressing the integrin  $\beta 3$  subunit alone or in combination with  $\alpha\text{IIb}$  on CHO cell adhesion to ATX-T210A. Although the parental CHO cell line did not adhere significantly to ATX, CHO cells expressing  $\beta 3$  integrins acquired the ability to inter-

act with ATX-T210A in the presence of the integrin activator  $\text{Mn}^{2+}$  (Fig. 2*D*). The interaction of CHO cells with ATX-T210A was specifically mediated by  $\beta 3$  integrins because it was completely blocked by 7E3 (Fig. 2*D*). Because integrin  $\beta 3$  associates with the widely expressed vitronectin  $\alpha$  subunit CHO cells (which do not express the platelet-specific  $\alpha\text{IIb}$  subunit), these observations also establish that ATX-T210A binds to  $\alpha\text{V}\beta 3$ , indicating that association with this integrin may account for ATX binding to other cell types.

Platelet integrins classically require agonist activation to recognize protein ligands. We therefore verified the agonist requirements for ATX-T210A binding to platelets. Agonists that act through G-protein-coupled receptors, including ADP, the PAR1 thrombin receptor-activating peptide (TRAP), and thrombin, as well as a non-G-protein-coupled receptor pathway (collagen), all promoted platelet adhesion to ATX-T210A (Fig. 3*A*). ADP-promoted platelet adhesion to ATX-T210A was attenuated by the P2Y12 receptor antagonist cangrelor and the P2Y1 antagonist MRS-2719 (Fig. 3*B*). Cangrelor and ADPase (apyrase) also inhibited adhesion of TRAP-stimulated platelets to ATX (Fig. 3*B*), identifying a role for released ADP in PAR1-stimulated platelet adhesion to ATX-T210A (Fig. 3*B*). In keeping with known mechanisms of integrin activation, ADP-stimulated platelet adhesion to ATX was inhibited by pretreatment of platelets with forskolin to elevate intraplatelet cAMP and was partially reduced by inhibitors of protein kinase A (PKI(14–

## Regulation of Autotaxin by Integrin Binding

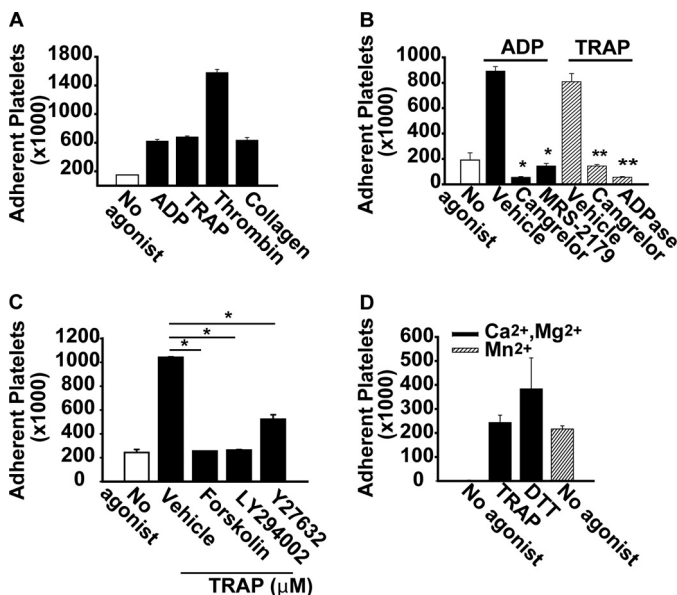


**FIGURE 3. Platelet binding to ATX requires agonist activation of integrins.** *A*, gel-filtered calcein-labeled platelets (200,000/ $\mu$ l in Tyrode's buffer with 2 mM  $\text{CaCl}_2$  and 1 mM  $\text{MgCl}_2$ ) were incubated with microtiter wells containing ATX-T210A (immobilized at 5  $\mu$ g/ml) in the absence of agonist (*open bar*) or in the presence of 10  $\mu$ M ADP, 15  $\mu$ M TRAP, 0.5 units/ml thrombin, or 10  $\mu$ g/ml collagen for 1 h at 37  $^\circ\text{C}$ . After washing the wells three times, platelet adhesion was quantitated by determining fluorescence associated with the wells. *B*, platelets were incubated in microtiter wells containing immobilized ATX in the absence of agonist (*open bar*) or presence of ADP (*closed bars*) or TRAP (*hatched bars*). Where indicated, 0.5  $\mu$ M cangrelor (P2Y12 antagonist), 10  $\mu$ M MRS-2179 (P2Y1 antagonist), or 1 units/ml apyrase (*ADPase*) was included in the assay. \*,  $p < 0.05$  versus ADP/vehicle, ANOVA; \*\*,  $p < 0.05$  versus TRAP/vehicle, ANOVA. *C*, platelets were incubated with wells with immobilized ATX in the absence of agonist or presence of ADP and with either 100  $\mu$ M forskolin, 20  $\mu$ M LY294002 (PI3K inhibitor), or 2.5  $\mu$ M Y27632 (Rho kinase inhibitor). \*,  $p < 0.05$  versus vehicle, ANOVA. *D*, platelets (in Tyrode's buffer with the indicated divalent cations) were incubated in microtiter wells containing ATX with vehicle (no agonist), 15  $\mu$ M TRAP, 2.5  $\mu$ M DTT, or 50  $\mu$ M  $\text{Mn}^{2+}$ . Results are presented as the number of adherent platelets (mean  $\pm$  S.D.) from at least three independent experiments performed in triplicate.

22)), PI3K (LY294002), or Rho kinase (Y27632) (Fig. 3C). In addition to classic platelet agonists, the direct integrin activator  $\text{Mn}^{2+}$  and treatment of platelets with the reducing agent DTT, which stimulates the adhesive function of several integrins, resulted in agonist-independent adhesion to ATX (Fig. 3D).

The preceding observations of ATX binding to integrins on platelets and mammalian cells employed microtiter plate assays with immobilized ATX. We next investigated binding of soluble  $^{125}\text{I}$ -labeled ATX to platelets in suspension. When  $^{125}\text{I}$ -ATX and unlabeled ATX were incubated at various ratios while maintaining the total ATX concentration constant, a linear relationship was observed between the percent  $^{125}\text{I}$ -ATX bound and the percent added (Fig. 4A), indicating that radiolabeling of ATX did not affect the protein's ability to recognize platelets. Binding of  $^{125}\text{I}$ -ATX to activated platelets was time-dependent and saturable (Fig. 4, B and C). Scatchard analysis of data obtained using an excess of unlabeled ATX to define non-specific binding revealed an affinity of  $\sim 300$  nM and a maximal number of  $\sim 75,000$  ATX-binding sites/platelet. Addition of excess echistatin partially displaced bound  $^{125}\text{I}$ -ATX (Fig. 4B), suggesting that at least some of the ATX remained on the platelet surface after 30 min. Inclusion of fibrinogen in the reaction

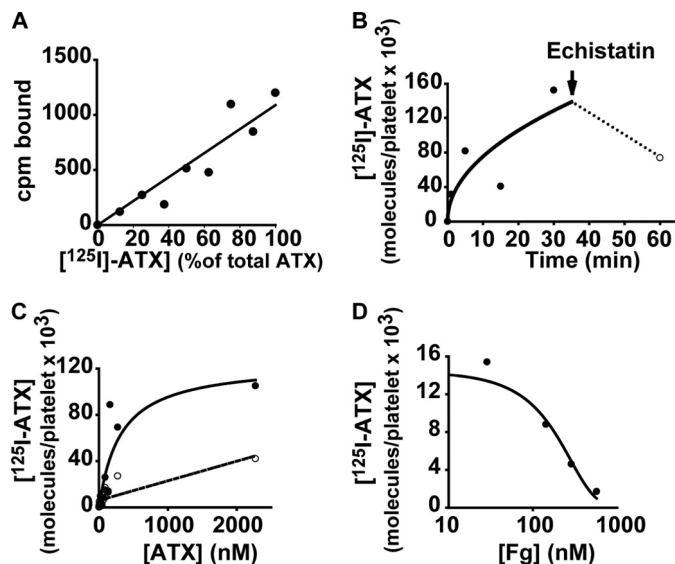


**FIGURE 4. Affinity and stoichiometry of  $^{125}\text{I}$ -ATX binding to activated platelets.** *A*, 15  $\mu$ M TRAP-activated platelets (200,000/ $\mu$ l) were incubated with a total of 73 nM ATX, composed of varying amounts of  $^{125}\text{I}$ -labeled ATX and unlabeled ATX, and platelet-bound ATX was determined as described under "Experimental Procedures." *B*, TRAP-activated platelets were incubated with  $^{125}\text{I}$ -ATX for the indicated times. At 30 min, echistatin (20  $\mu$ g/ml) was added, and incubations were continued for an additional 30 min to determine reversibility. *C*, TRAP-activated platelets (●) or resting platelets (○) were incubated with the indicated concentrations of ATX for 30 min. *D*, TRAP-activated platelets were incubated with  $^{125}\text{I}$ -ATX in the presence of the indicated concentrations of fibrinogen (*Fg*). Data are means of duplicate determinations.

dose-dependently blocked  $^{125}\text{I}$ -ATX binding to platelets with a  $K_i$  of 220 nM (Fig. 4D).

*lyso-PLD-independent Effects of ATX on Platelet Aggregation and Adhesion*—ATX is a monomeric protein in solution (16) and would not be expected to support platelet aggregation, which requires cross-linking of at least two binding sites on adjacent platelets. Under conditions where ADP-induced aggregation of washed platelets was enhanced by addition of exogenous fibrinogen, inclusion of soluble ATX-T210A did not further enhance platelet aggregation (Fig. 5A). In fact, the maximal extent of aggregation of platelets was moderately lower in the presence of ATX-T210A (Fig. 5, A and B, left panel). The ability of ATX-T210A to reduce platelet aggregation varied between platelet preparations from different donors (Fig. 5B, right panel), but the extent of aggregation was consistently lower in the presence of ATX-T210A. Together, these observations and the fact that fibrinogen competes for soluble ATX binding (Fig. 3D) are consistent with a model in which ATX and fibrinogen interact with a mutually accessible binding site(s) on platelets but only fibrinogen supports platelet aggregation.

ATX exerts a counter-adhesive effect on oligodendrocytes that is consistent with inhibition of integrin-dependent adhesion and signaling (26). ATX may also be capable of hydrolyzing nucleotides along the platelet surface and thereby impact signaling events. The inhibitory effects of ATX on platelet aggregation were independent of catalytic activity because inactive ATX-T210A also inhibited aggregation. Nonetheless, we sought to determine whether ATX has direct inhibitory effects on platelet function by determining whether ATX would alter adhesion to fibrinogen immobilized at submaximal concentra-

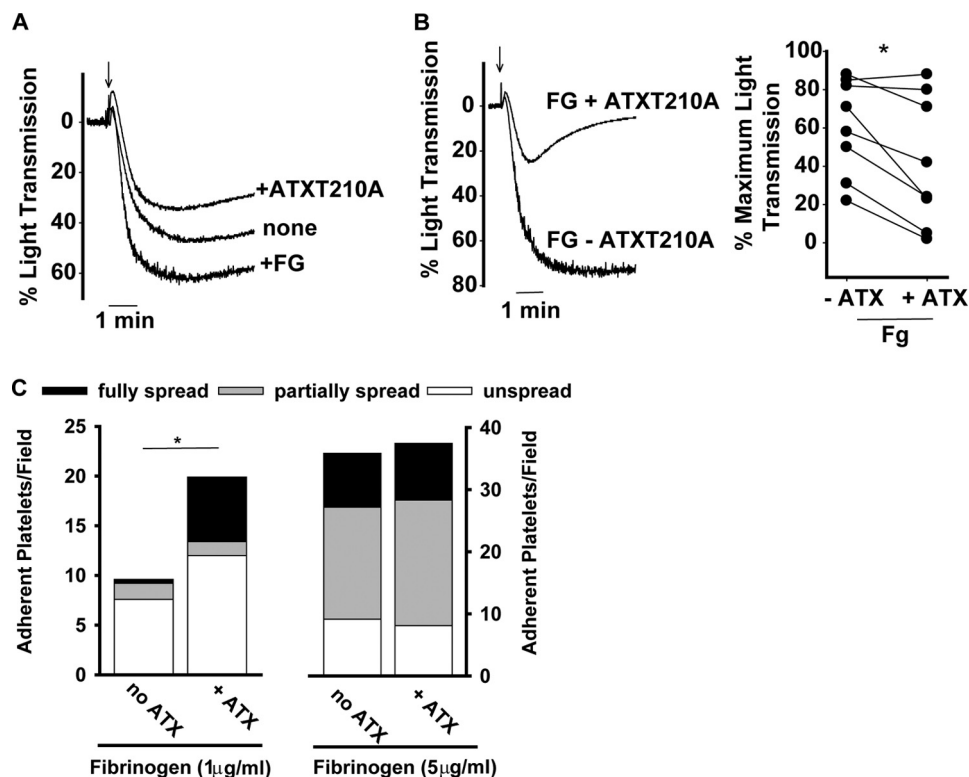


**FIGURE 5. Effects of ATX on fibrinogen-dependent platelet aggregation and adhesion.** *A*, gel-filtered platelets ( $200,000/\mu\text{l}$ ) were stirred in the absence or presence of  $200 \mu\text{g/ml}$  fibrinogen (+FG) or  $50 \mu\text{g/ml}$  ATX-T210A (+ATX). Platelet aggregation was stimulated by the addition of  $15 \mu\text{M}$  TRAP at the time indicated by the arrow. *B*, gel-filtered platelets ( $200,000/\mu\text{l}$ ) stirred in the presence of  $200 \mu\text{g/ml}$  fibrinogen without ATX (FG - ATX) or with  $50 \mu\text{g/ml}$  ATX (FG + ATX).  $15 \mu\text{M}$  TRAP was added at the time indicated by the arrow. *Left panel*, representative light transmission tracing from single donor; *right panel*, cumulative maximal percent aggregation from different donors (\*,  $p < 0.05$ , paired *t* test). *C*, platelets ( $20,000/\mu\text{l}$ ) were incubated with wells precoated with either 1 or  $5 \mu\text{g/ml}$  fibrinogen in the presence or absence of  $5 \mu\text{g/ml}$  ATX. Adherent platelets were stained with TRITC-phalloidin, and the total number of platelets/field in 4–5 fields was counted. Where indicated, the number of platelets adherent in the presence of soluble ATX was also determined. The platelets in each field were scored as fully spread (defined by the presence of cortical actin reorganization), partially spread (presence of filopodia), or not spread (neither cortical actin or filopodia). \*,  $p < 0.05$ , *t* test.

tions (low density;  $1 \mu\text{g/ml}$ ). In the absence of agonists, platelets adhere to low density fibrinogen, and the adhesion triggers platelet activation (31, 32). In agreement with our aggregation studies, soluble ATX blocked platelet adhesion to immobilized fibrinogen by 70% (from  $9.6 \pm 2.0$  to  $2.8 \pm$  platelets/high powered field). However, more platelets adhered to surfaces containing both immobilized fibrinogen and ATX than to surfaces containing fibrinogen alone ( $20 \pm 5$  versus  $9.6 \pm 2$  platelets/high powered field; Fig. 5C, left). In addition, more platelets spread on surfaces with immobilized fibrinogen and ATX than spread on surfaces containing immobilized fibrinogen alone (Fig. 5C, left). These results suggest that fibrinogen binding may promote “outside-in” signaling necessary for platelets to recognize ATX. When fibrinogen was immobilized at higher density concentrations ( $5 \mu\text{g/ml}$ ) that are known to promote maximal platelet activation and adhesion (31, 32), the inclusion of immobilized ATX did not inhibit adhesion or spreading (Fig. 5C, right). Thus, rather than negatively affecting the adhesive function of platelet integrins, as has been observed in experiments with oligodendrocytes, ATX moderately facilitates platelet adhesion to fibrinogen.

**Tandem SMB Domains Are the Sole ATX-binding Sites for  $\beta_3$  Integrins**—We next sought to identify the motifs in ATX responsible for interacting with platelets. ATX contains an arginine, glycine, aspartic acid (RGD) sequence motif within

the second SMB-like domain (Fig. 6, A and B). Because this motif confers integrin binding to other proteins, including the structurally related SMB-like domain of vitronectin, we surmised that it would perform a similar function in ATX. Surprisingly, the ATX crystal structure revealed that the RGD motif amino acids are incompletely solvent-exposed. In agreement, we found that nonconservative substitutions of the RGD residues did not abolish integrin binding.<sup>4</sup> However, in the course of these studies, we found that mutation of a charged, surface-exposed residue at the N terminus of the ATX SMB2 domain significantly reduced binding of ATX to platelet integrins, identifying an important role for the SMB2 domain in this process (17). To determine whether the SMB2 domain is the sole integrin-binding site on ATX and begin to explore interactions of ATX with integrins on other cells, we compared binding of an ATX fragment containing the tandem SMB domains to CHO cells expressing human integrin  $\beta_3$ . Binding of these cells to the SMB domain fragment was promoted by the integrin activator  $\text{Mn}^{2+}$  and inhibited by 7E3 in an identical manner to that of wild type ATX, indicating that the SMB domains (and not the PDE and nuclease-like domains) account for ATX binding to  $\beta_3$  integrins (Fig. 6, C and D).

<sup>4</sup> A. J. Morris, unpublished observations.

## Regulation of Autotaxin by Integrin Binding

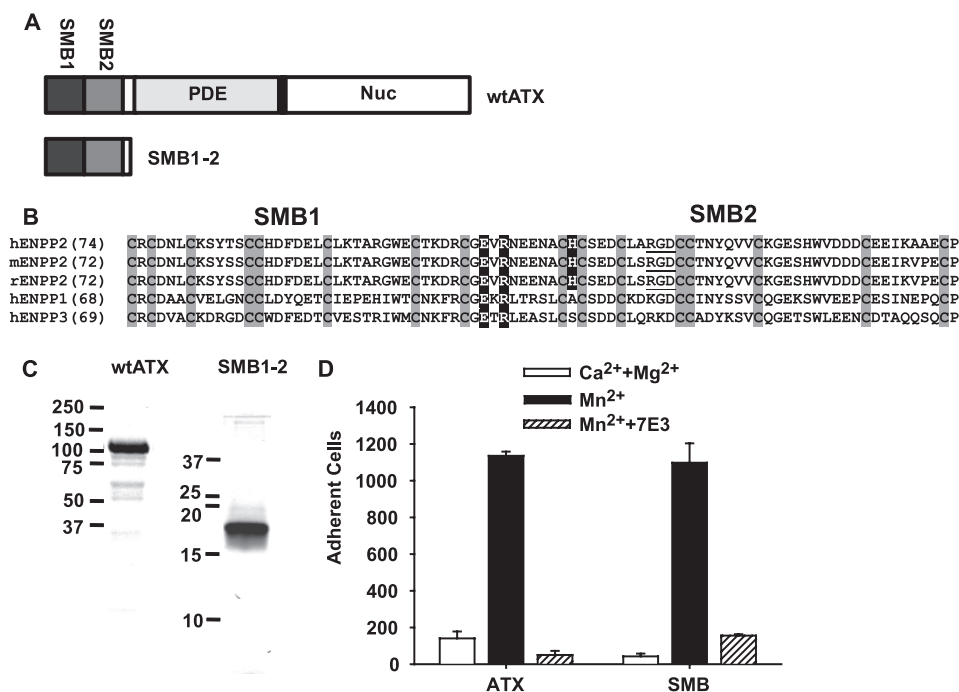


**FIGURE 6. N-terminal tandem SMB domain is the sole ATX integrin-binding site.** *A*, domain structure of ATX and the N-terminal tandem SMB domain fragment. *Nuc*, nuclease-like domain *B*, sequence alignment of the SMB1 and SMB2 domains of human, rat, and mouse ENPP2 (ATX) and ENPP1 and ENPP3 with the RGD sequence underlined, cysteine residues boxed in *gray*, and charged residues targeted for mutation boxed in *black*. *C*, analysis of purified recombinant wild type ATX (*wtATX*) and the N-terminal tandem SMB domain fragment (*SMB1-2*) by SDS-PAGE and staining with Coomassie Blue. *D*, CHO cells stably expressing the human  $\beta 3$  integrin subunit were incubated with immobilized ATX or the N-terminal SMB1-2 fragment in the presence of 2 mM CaCl<sub>2</sub> and 1 mM MgCl<sub>2</sub> (*open bars*), 50  $\mu$ M MnCl<sub>2</sub> (*black bars*), or 50  $\mu$ M MnCl<sub>2</sub> and 20  $\mu$ g/ml of the function-blocking integrin  $\beta 3$  antibody 7E3 (*hatched bars*). Data shown are means  $\pm$  S.D. of triplicate determinations.

*ATX Binding to Platelet Integrins Enables Agonist-stimulated LPA Production*—Having established the properties of ATX binding to  $\beta 3$  integrins, we used platelets and CHO cell systems to test the hypothesis that integrin-mediated recruitment of ATX to the outer face of the plasma membrane enables localized LPA production. To investigate this possibility, we measured the rate of hydrolysis of BSA-bound C17-LPC in the presence of either the parental CHO cells or the  $\alpha$ IIb $\beta$ 3-expressing CHO cells using Mn<sup>2+</sup> as the integrin activator. Under conditions where, based on our measurements of the affinity of platelet  $\alpha$ IIb $\beta$ 3 for ATX, all of the added ATX would be bound to the integrin, we observed an  $\sim$ 2-fold increase in ATX activity in the presence of integrin-expressing cells (Fig. 7A). These results suggest that integrin binding increases ATX activity against exogenous substrates. Our experiments with activated platelets indicated that integrin-bound ATX could act on endogenously generated lysophospholipid substrates. Although like resting platelets, parental, and  $\alpha$ IIb $\beta$ 3-expressing CHO cells contained readily detectable LPC, we did not observe significant production of LPA when they were incubated with ATX (data not shown). However, we found that preincubation of these cells with bee venom PLA<sub>2</sub> increased cell-associated LPC levels  $\sim$ 2-fold (Fig. 7B), which presumably reflects the previously described ability of this enzyme to promote LPC-dependent responses when added exogenously to mammalian cells (35). Under these conditions, ATX elicited concentration-dependent increases in cell-associated LPA, and at lower concentrations of ATX, LPA production was increased  $\sim$ 4-fold by overexpression of  $\alpha$ IIb $\beta$ 3 (Fig. 7C). The effect of ATX was

substantially attenuated when the integrin-blocking antibody 7E3 was included in these incubations (Fig. 7D). Although the parental CHO cell line failed to bind to ATX appreciably in the static adhesion assay (Fig. 2), these results suggest that relatively low levels of integrin binding are sufficient to sustain significant production of LPA by cell-associated ATX.

The crystal structures reported are of rodent ATX orthologs (17, 18). We made variants of human ATX with nonconservative substitutions of charged surface-exposed residues in the SMB2 domain, including H117A, which corresponds to H119A of the rodent sequence and was previously shown to exhibit decreased binding to platelet  $\beta 3$  integrins (Fig. 8A and also see Fig. 6 for sequence details) (17). We examined catalytic activity of these variants against mixed micelles of Triton X-100 and 18:0 LPC. The apparent  $K_m$  and  $V_{max}$  values for LPC of these SMB domain mutants were very similar to that of wild type ATX, indicating that mutation of the SMB2 domain does not impair catalytic activity against detergent-solubilized substrates (Fig. 8B). Activity of these variants against the small molecule substrate bis-paranitrophenol phosphate was also indistinguishable from wild type ATX (data not shown). We examined binding of these ATX SMB2 domain variants to  $\beta 3$  integrin-expressing CHO cells. Binding of these cells to ATX H117A (as expected) and ATX E109A but not ATXR117A was significantly lower than to wild type ATX (Fig. 8C). We then compared the ability of wild type ATX and ATX E109A to increase LPA production when incubated with thrombin-stimulated platelets. Although wild type ATX produced a robust increase in LPA production, ATX E109A did not, indicating

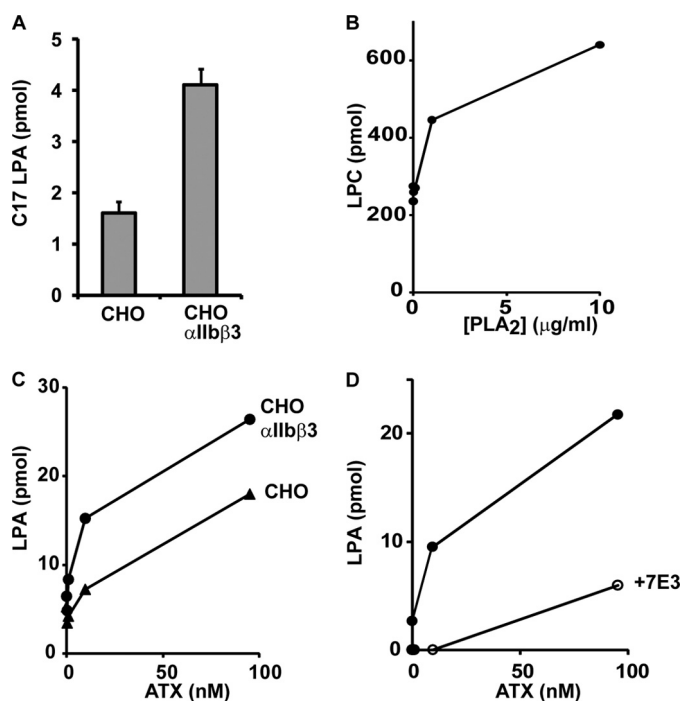


**FIGURE 7. ATX activity against exogenously provided and cell-associated substrates is increased by integrin binding.** *A*, control or  $\alpha$ IIb $\beta$ 3 expressing CHO cells were incubated with 100 nM ATX in Tyrode's buffer containing 1 mM MgCl<sub>2</sub>, 50  $\mu$ M MnCl<sub>2</sub>, 100  $\mu$ M C17 LPC, and 0.35% BSA. Production of C17 LPA was measured after a 1-h incubation at 37 °C. *B*, CHO cells were incubated with increasing concentrations of bee venom PLA<sub>2</sub> and total cell-associated levels of 15 abundant LPC species were determined. *C*, control or  $\alpha$ IIb $\beta$ 3-expressing CHO cells were preincubated with bee venom PLA<sub>2</sub> and then incubated with the indicated concentrations of ATX in the Tyrode's buffer used for the experiment shown in *A*, omitting the C17 LPC, and production of LPA was determined as described under "Experimental Procedures." *D*,  $\alpha$ IIb $\beta$ 3-expressing CHO cells were preincubated with bee venom PLA<sub>2</sub> and then incubated with the indicated concentrations of ATX in the Tyrode's buffer in the presence or absence of 10  $\mu$ g/ml of the integrin blocking antibody 7E3 and production of LPA determined as described under "Experimental Procedures." The data shown are means  $\pm$  S.D. of triplicate determinations (*A*) or duplicate determinations (*B*–*D*).

that association with  $\beta$ 3 integrins is important for this process (Fig. 8D).

## DISCUSSION

LPA is produced and degraded by multiple pathways and also serves as an intermediate in the *de novo* synthesis of phospholipids. In this study, we describe a mechanism by which the metabolic and signaling functions of LPA can be delimited by localizing LPA production to the cell surface through recruitment to activated integrin receptors. We used human platelets as a model system to dissect the regulation and specificity of integrin binding to ATX. We found that a disparate variety of platelet agonists promote ATX binding to platelets. The ability of agonists to stimulate ATX binding appears to be strongly dependent on ADP signaling through the P2Y<sub>12</sub> purinergic receptor, as evidenced by the ability of cangrelor and apyrase to inhibit TRAP-induced adhesion to immobilized ATX. The finding that forskolin treatment abolishes platelet adhesion to ATX is also consistent with a role for P2Y<sub>12</sub> signaling through G $\alpha_i$  to decrease platelet cAMP levels as an important component of the signaling pathway response. Stimulation of platelet adhesion to ATX by Mn<sup>2+</sup> in the absence of agonists implicates

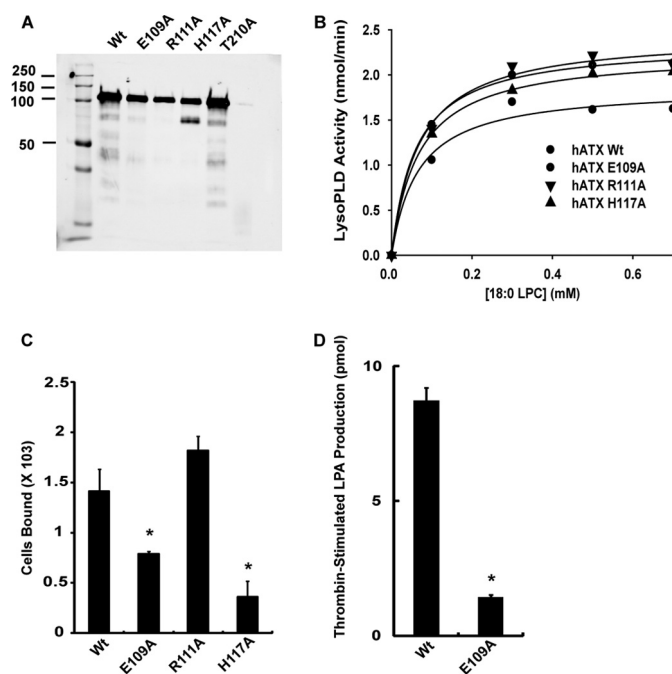


**FIGURE 8. ATX SMB2 mutants with impaired binding to  $\beta$ 3 integrins display reduced LPA generating capacity.** *A*, SDS-PAGE analysis of purified wild type ATX and the indicated variants. *B*, lyso-PLD activity of wild type ATX and the indicated variants determined using Triton X-100 solubilized 18:0 LPC. *C*, binding of  $\beta$ 3 integrin-expressing CHO cells to wild type ATX and the indicated ATX variants was determined as described under "Experimental Procedures" (mean  $\pm$  S.D. of triplicate determinations). *D*, effect of wild type ATX and ATX E019A on LPA production by thrombin-stimulated platelets was determined as described under "Experimental Procedures" (mean  $\pm$  S.D. of triplicate determinations).

integrins in this process, and studies using integrin-blocking antibodies and CHO cells expressing recombinant integrins indicate a role for  $\beta$ 3 integrins ( $\alpha$ IIb $\beta$ 3 and  $\alpha$ V $\beta$ 3) and to a lesser extent  $\beta$ 1 integrins in this process. The involvement of integrins in platelet binding to ATX is consistent with the density of ATX-binding sites/platelet observed with radiolabeled soluble ATX binding experiments. These results raise the possibility that, because  $\alpha$ V $\beta$ 3 and  $\beta$ 1 integrins are broadly expressed, cell surface recruitment of ATX through integrin binding may be a widespread phenomenon.

Consistent with this idea, binding of ATX to lymphocytes and oligodendrocytes has been reported previously (25, 26). In the latter system, ATX binding was shown to disrupt cell adhesion through a process that was postulated to involve antagonism of an unidentified adhesive receptor (26). We found that ATX impedes fibrinogen-dependent platelet aggregation. This is likely because ATX and fibrinogen compete for binding to the same integrin receptors but as ATX is a monovalent integrin ligand it cannot support platelet aggregation. Consistent with this idea, we found that fibrinogen competitively inhibited binding of soluble radiolabeled ATX to platelets. However, when ATX and fibrinogen were immobilized together at submaximal concentrations, we found that ATX modestly enhanced, rather than inhibited, adhesion. Thus, unlike ATX binding to oligodendrocytes, which appears to trigger signals that inhibit other adhesive events, our results are consistent with a model in which fibrinogen and ATX compete for the same binding sites on platelets. Our prior observation that ATX



## Regulation of Autotaxin by Integrin Binding

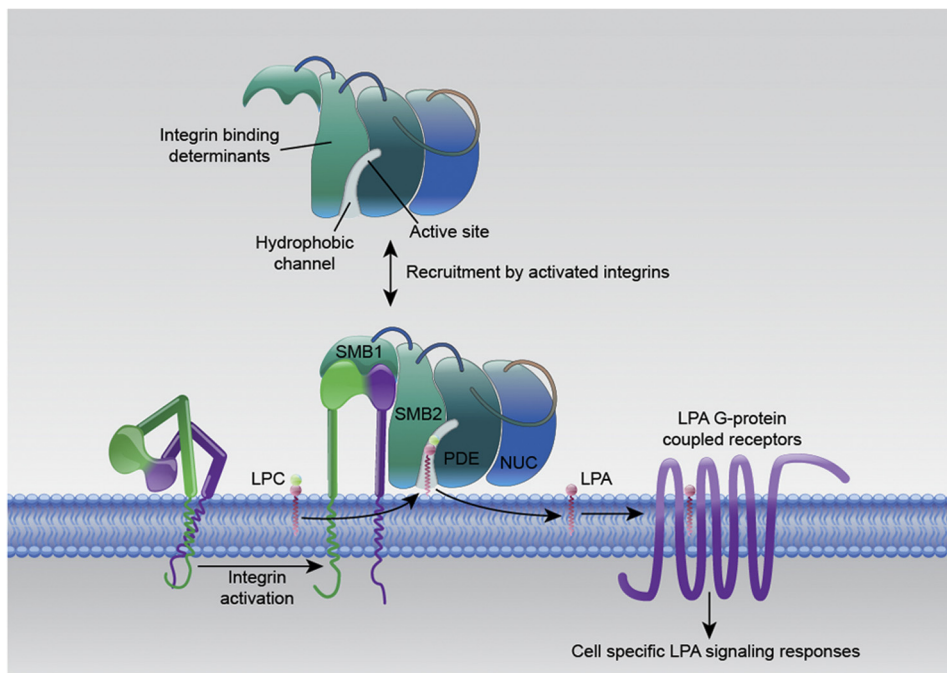


FIGURE 9. Recruitment of ATX to the cell surface by activated integrins enables localized production of LPA by hydrolysis of cell surface lysophospholipid substrates.

is recruited to thrombus *in vivo* suggests that the interaction of ATX with activated platelet integrins we have characterized here *in vitro* occurs physiologically (11). In *in vitro* assays, ATX displays nucleotide pyrophosphatase/phosphodiesterase activity. It is possible that localization of ATX along the platelet surface provides a mechanism for degradation of released ATP (a platelet inhibitor) and ADP (a platelet activator). To date, however, we have been unable to detect an impact of ATX on circulating nucleotides (27).

Efforts to define the physiological role of LPA signaling in platelet function have been confounded by observations of heterogeneity in human platelet responses to LPA and the fact that, although LPA is a weak agonist for human platelets from most donors, it does not activate rodent platelets (4, 6). However, several lines of evidence implicate platelets as important participants in the production of LPA in whole blood *ex vivo* and in mouse models (20, 23). We found that a recently described potent small molecule ATX inhibitor completely attenuated production of LPA by thrombin-stimulated washed platelets. The delipidated BSA used in these incubations contained trace levels of LPC that were less than 1% of the quantity of LPA being generated, so clearly these results indicate that endogenous ATX acting on endogenously formed LPC is responsible for producing LPA in this system. Addition of purified ATX to washed platelets at concentrations in the range of  $\sim 100$  nM, which are in line with those present in plasma, resulted in dramatically enhanced sustained production of LPA by thrombin-stimulated washed platelets. We also found that ATX could hydrolyze CHO cell-associated lysophospholipids and that this activity was substantially enhanced when cells expressing integrin  $\beta 3$  were used as the source of substrate. In such experiments, a concentration in the range of 1–10 nM ATX achieved half of the maximal LPA levels. Small differences

in levels to achieve maximal LPA levels (Fig. 7, B and C) may be attributed to the slightly different levels of purity between different preparations of recombinant ATX, which results in slight differences in quantification of protein in different preparations. We identified the N-terminal ATX tandem SMB domain as sole site of integrin binding, and we generated point mutants in the SMB1 domain of ATX that exhibited parallel reductions in binding to  $\beta 3$  integrins and the ability to generate LPA when incubated with thrombin-stimulated platelets. Taken together, these results indicate that integrin binding to ATX brings the enzyme into close proximity with cell surface substrates that would generate LPA in the vicinity of its receptors (Fig. 9). Intriguingly, the ATX hydrophobic substrate binding channel through which cell surface substrates and products must enter and leave the active site is formed from the interface between the SMB and PDE domains (17, 18), raising the possibility that integrin binding might alter catalytic activity of the enzyme.

Although ATX can clearly generate LPA in blood plasma through hydrolysis of high concentrations of circulating LPC, and this activity is important for maintaining plasma LPA levels in the  $\geq 100$   $\mu\text{M}$  range in the face of rapid elimination (13, 14), very little is known about the extracellular concentration of LPA in tissues. Furthermore, although a role for circulating levels of the structurally related lipid mediator sphingosine 1-phosphate in control of the permeability of lymphatic and vascular endothelium is well supported by substantial data, the function of plasma LPA remains enigmatic (33). Our results suggest that the functions of circulating and cell-associated ATX are distinct. Recruitment of circulating ATX to activated platelets or the surface of vascular endothelial and vascular smooth muscle cells could lead to cell-specific LPA generation

and LPA signaling with important roles in vascular inflammation and injury responses (33).

Inhibition of LPA/ATX signaling is an attractive therapeutic target in cardiovascular disease in inflammation and cancer. To date, all of the inhibitors of ATX activity described, including several recently reported highly potent compounds, target the catalytic site of the enzyme to inhibit substrate binding or catalysis (13, 34). The ATX-integrin interaction reported here could be exploited to generate agents that selectively target ATX activity against cell-associated substrates. Indeed, antibody and small molecule inhibitors of integrin-ligand interactions have already been developed as anti-thrombotic and anti-cancer agents, and one compound of this type has been reported to alter LPA signaling involved in breast cancer metastasis in a mouse model (23). The possibility that some of the efficacy of these agents derives from inhibition of ATX recruitment to integrins warrants further examination.

*Acknowledgments*—We thank Tracy Drennan, Juliana Odetunde, and Marcielle de Beer for technical assistance and advice and Zhenyu Li, Barry Collier, and The Medicines Company for providing reagents.

## REFERENCES

- Choi, J. W., Herr, D. R., Noguchi, K., Yung, Y. C., Lee, C. W., Mutoh, T., Lin, M. E., Teo, S. T., Park, K. E., Mosley, A. N., and Chun, J. (2010) *Annu. Rev. Pharmacol. Toxicol.* **50**, 157–186
- Panetti, T. S., Hannah, D. F., Avraamides, C., Gaughan, J. P., Marcinkiewicz, C., Huttenlocher, A., and Mosher, D. F. (2004) *J. Thromb. Haemost.* **2**, 1654–1656
- Rizza, C., Leitinger, N., Yue, J., Fischer, D. J., Wang, D. A., Shih, P. T., Lee, H., Tigyi, G., and Berliner, J. A. (1999) *Lab. Invest.* **79**, 1227–1235
- Siess, W., Zangl, K. J., Essler, M., Bauer, M., Brandl, R., Corrinth, C., Bittman, R., Tigyi, G., and Aepfelbacher, M. (1999) *Proc. Natl. Acad. Sci. U.S.A.* **96**, 6931–6936
- Hayashi, K., Takahashi, M., Nishida, W., Yoshida, K., Ohkawa, Y., Kitabatake, A., Aoki, J., Arai, H., and Sobue, K. (2001) *Circ. Res.* **89**, 251–258
- Pamuklar, Z., Lee, J. S., Cheng, H. Y., Panchatcharam, M., Steinhubl, S., Morris, A. J., Charnigo, R., and Smyth, S. S. (2008) *Arterioscler. Thromb. Vasc. Biol.* **28**, 555–561
- Subramanian, P., Karshovska, E., Reinhard, P., Megens, R. T., Zhou, Z., Akhtar, S., Schumann, U., Li, X., van Zandvoort, M., Ludin, C., Weber, C., and Schober, A. (2010) *Circ. Res.* **107**, 96–105
- Panchatcharam, M., Miriyala, S., Yang, F., Rojas, M., End, C., Vallant, C., Dong, A., Lynch, K., Chun, J., Morris, A. J., and Smyth, S. S. (2008) *Circ. Res.* **103**, 662–670
- Zhou, Z., Subramanian, P., Sevilimis, G., Globke, B., Soehnlein, O., Karshovska, E., Megens, R., Heyll, K., Chun, J., Saulnier-Blache, J. S., Reinholz, M., van Zandvoort, M., Weber, C., and Schober, A. (2011) *Cell Metab.* **13**, 592–600
- Baker, D. L., Desiderio, D. M., Miller, D. D., Tolley, B., and Tigyi, G. J. (2001) *Anal. Biochem.* **292**, 287–295
- Pamuklar, Z., Federico, L., Liu, S., Umezū-Goto, M., Dong, A., Panchatcharam, M., Fulkerson, S., Fulerson, Z., Berdyshev, E., Natarajan, V., Fang, X., van Meeteren, L. A., Moolenaar, W. H., Mills, G. B., Morris, A. J., and Smyth, S. S. (2009) *J. Biol. Chem.* **284**, 7385–7394
- Umezū-Goto, M., Kishi, Y., Taira, A., Hama, K., Dohmae, N., Takio, K., Yamori, T., Mills, G. B., Inoue, K., Aoki, J., and Arai, H. (2002) *J. Cell Biol.* **158**, 227–233
- Albers, H. M., Dong, A., van Meeteren, L. A., Egan, D. A., Sunkara, M., van Tilburg, E. W., Schuurman, K., van Tellingen, O., Morris, A. J., Smyth, S. S., Moolenaar, W. H., and Ova, H. (2010) *Proc. Natl. Acad. Sci. U.S.A.* **107**, 7257–7262
- Tomsig, J. L., Snyder, A. H., Berdyshev, E. V., Skobeleva, A., Mataya, C., Natarajan, V., Brindley, D. N., and Lynch, K. R. (2009) *Biochem. J.* **419**, 611–618
- Stefan, C., Jansen, S., and Bollen, M. (2005) *Trends Biochem. Sci.* **30**, 542–550
- Tokumura, A., Majima, E., Kariya, Y., Tominaga, K., Kogure, K., Yasuda, K., and Fukuzawa, K. (2002) *J. Biol. Chem.* **277**, 39436–39442
- Hausmann, J., Kamtekar, S., Christodoulou, E., Day, J. E., Wu, T., Fulkerson, Z., Albers, H. M., van Meeteren, L. A., Houben, A. J., van Zeijl, L., Jansen, S., Andries, M., Hall, T., Pegg, L. E., Benson, T. E., Kasiem, M., Harlos, K., Kooi, C. W., Smyth, S. S., Ova, H., Bollen, M., Morris, A. J., Moolenaar, W. H., and Perrakis, A. (2011) *Nat. Struct. Mol. Biol.* **18**, 198–204
- Nishimasu, H., Okudaira, S., Hama, K., Mihara, E., Dohmae, N., Inoue, A., Ishitani, R., Takagi, J., Aoki, J., and Nureki, O. (2011) *Nat. Struct. Mol. Biol.* **18**, 205–212
- Tabchy, A., Tigyi, G., and Mills, G. B. (2011) *Nat. Struct. Mol. Biol.* **18**, 117–118
- Aoki, J., Taira, A., Takanezawa, Y., Kishi, Y., Hama, K., Kishimoto, T., Mizuno, K., Saku, K., Taguchi, R., and Arai, H. (2002) *J. Biol. Chem.* **277**, 48737–48744
- Tigyi, G., and Miledi, R. (1992) *J. Biol. Chem.* **267**, 21360–21367
- Eichholtz, T., Jalink, K., Fahrenfort, L., and Moolenaar, W. H. (1993) *Biochem. J.* **291**, 677–680
- Boucharaba, A., Serre, C. M., Grès, S., Saulnier-Blache, J. S., Bordet, J. C., Guglielmi, J., Clézardin, P., and Peyruchaud, O. (2004) *J. Clin. Invest.* **114**, 1714–1725
- Bolen, A. L., Naren, A. P., Yarlagadda, S., Beranova-Giorgianni, S., Chen, L., Norman, D., Baker, D. L., Rowland, M. M., Best, M. D., Sano, T., Tsukahara, T., Liliom, K., Igarashi, Y., and Tigyi, G. (2011) *J. Lipid Res.* **52**, 958–970
- Kanda, H., Newton, R., Klein, R., Morita, Y., Gunn, M. D., and Rosen, S. D. (2008) *Nat. Immunol.* **9**, 415–423
- Fox, M. A., Colello, R. J., Macklin, W. B., and Fuss, B. (2003) *Mol. Cell Neurosci.* **23**, 507–519
- Federico, L., Pamuklar, Z., Smyth, S. S., and Morris, A. J. (2008) *Curr. Drug Targets* **9**, 698–708
- Sano, T., Baker, D., Virag, T., Wada, A., Yatomi, Y., Kobayashi, T., Igarashi, Y., and Tigyi, G. (2002) *J. Biol. Chem.* **277**, 21197–21206
- Nakamura, K., Igarashi, K., Ide, K., Ohkawa, R., Okubo, S., Yokota, H., Masuda, A., Oshima, N., Takeuchi, T., Nangaku, M., Okudaira, S., Arai, H., Ikeda, H., Aoki, J., and Yatomi, Y. (2008) *Clin. Chim. Acta* **388**, 51–58
- Smyth, S. S., Sciorra, V. A., Sigal, Y. J., Pamuklar, Z., Wang, Z., Xu, Y., Prestwich, G. D., and Morris, A. J. (2003) *J. Biol. Chem.* **278**, 43214–43223
- Collier, B. S., Kutok, J. L., Scudder, L. E., Galanakis, D. K., West, S. M., Rudomen, G. S., and Springer, K. T. (1993) *J. Clin. Invest.* **92**, 2796–2806
- Jirousková, M., Jaiswal, J. K., and Collier, B. S. (2007) *Blood* **109**, 5260–5269
- Smyth, S. S., Cheng, H. Y., Miriyala, S., Panchatcharam, M., and Morris, A. J. (2008) *Biochim. Biophys. Acta* **1781**, 563–570
- Gierse, J., Thorarensen, A., Beltey, K., Bradshaw-Pierce, E., Cortes-Burgos, L., Hall, T., Johnston, A., Murphy, M., Nemirovskiy, O., Ogawa, S., Pegg, L., Pelc, M., Prinsen, M., Schnute, M., Wendling, J., Wene, S., Weinberg, R., Wittwer, A., Zweifel, B., and Masferrer, J. (2010) *J. Pharmacol. Exp. Ther.* **334**, 310–317
- Perrin-Cocon, L., Agaagué, S., Coutant, F., Masurel, A., Bezzine, S., Lambeau, G., André, P., and Lotteau, V. (2004) *Eur. J. Immunol.* **34**, 2293–2302